ORIGINAL PAPER

Molecular interactions between mitochondrial membrane proteins and the C-terminal domain of PB1-F2: an in silico approach

Mohd Danishuddin · Shahper N. Khan · Asad U. Khan

Abstract PB1-F2 is a recently described influenza A viral protein that induces apoptosis by binding with two mitochondrial membrane proteins, i.e. VDAC1 (outer membrane) and ANT3 (inner membrane). Knowledge of this binding mechanism could provide insights that would aid in the design of novel inhibitors against this protein. Therefore, to better understand these interactions, we have undertaken this study to model the PB1-F2 protein of the highly pathogenic influenza A virus subtype H5N1. Moreover, a model of human ANT3 was also established. The dynamics of the molecular interactions between the C-terminal region of PB1-F2 protein and VDAC1 and ANT3 were expounded by employing an in silico approach. Our results suggest the involvement of 12 amino acids of PB1-F2 protein, which form hydrophobic contacts with 22 amino acids of VDAC1. Of these, Leu64, Arg75 and Val76 were found to be crucial for mitochondrial targetting. In the case of the PB1-F2-ANT3 complex, 14 amino acids of ANT3 were found to make hydrophobic contacts with 9 amino acids of PB1-F2. Furthermore, two hydrogen bonds were predicted in both complexes PB1-F2/VDAC1 and PB1-F2/ANT3. This study reveals the molecular interactions required for PB1-F2-induced apoptosis and suggests a hypothetical model for future study.
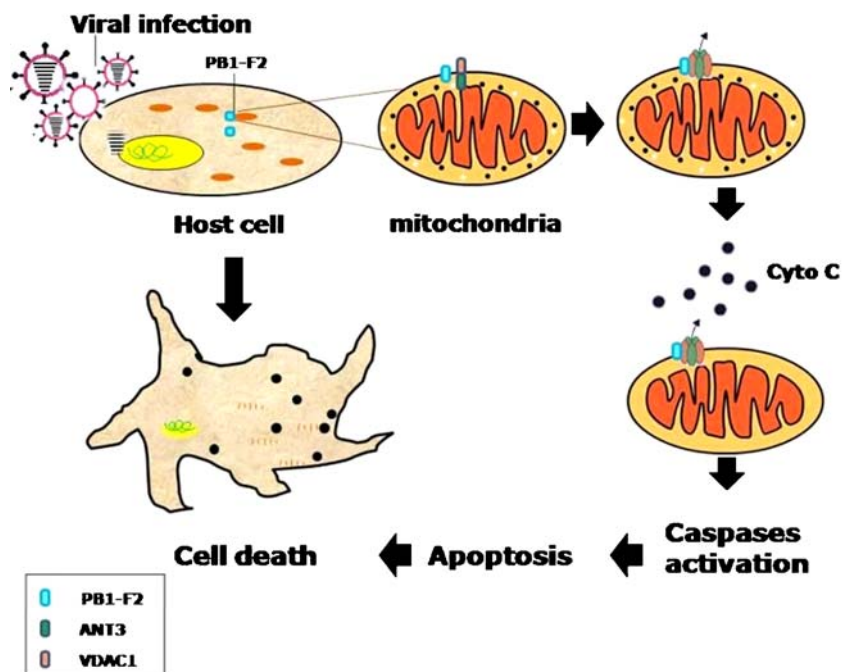
Keywords PB1-F2 · Homology modelling · Protein–protein interaction · VDAC1 · ANT3

M. Danishuddin · S. N. Khan · A. U. Khan (✉)
Interdisciplinary Biotechnology Unit, Aligarh Muslim University,
Aligarh 202002, India
e-mail: asad.k@rediffmail.com
e-mail: asadukhan72@gmail.com

Introduction

Influenza A viruses (IAV) are important pathogens, threatening both humans and animals worldwide. IAVs, which belong to the orthomyxoviridae family, consist of eight segments of negative sense RNA [1]. In 2001, a novel 87-amino acid protein, PB1-F2, from an alternative reading frame on polymerase basic protein 1 (PB1) in A/Puerto Rico/8/34 (H1N1) was characterised [2]. This protein is known to be short lived and to be expressed about 5 h post infection [2, 3]. The majority of IAV subtypes have the PB1-F2 open reading frame, whereas this ORF was found to be absent in influenza B viruses [2]. The function of this novel protein was to locate to the mitochondria of the infected cell and promote apoptosis through interaction with two mitochondrial membrane proteins: inner ANT3 (adenine nucleotide translocator 3) and outer VDAC1 (voltage dependent anion channel 1) [3, 4]. The interaction of PB1-F2 with these mitochondrial membrane proteins promotes the permeabilisation of the mitochondria and release of cytochrome c, which stimulates the cell (Fig. 1). These two mitochondrial membrane proteins are known to be critical components of the pore complex [3]. ANT3 is known to be an ATP/ADP carrier protein on the inner membrane of the mitochondria. It is believed that ANT3 and VDAC1 proteins undergo major conformational changes after interacting with the PB1-F2 protein, which leads to the formation of pores (ANT3 form pores on the inner membrane and VDAC1 form pores on the outer membrane). PB1-F2 protein contains two structured domains at the N- and C-termini, connected by flexible hinge regions. VDAC1, an outer membrane mitochondrial protein, interacts with both the N and C- terminal domains of the PB1-F2 protein. However, the positively charged basic amphipathic alpha helix in the C-terminal region of

the PB1-F2 protein is known to interact with inner membrane proteins [5, 6]. Although the role of this novel protein has been identified, its mechanism of mitochondrial targeting is still to be fully elucidated. Hence, in the present study we used in silico docking and structure refinement techniques to identify the amino acids and forces involved in stabilising the molecular interaction of PB1-F2 with the two mitochondrial membrane proteins ANT3 and VDAC1.

Materials and methods

Data sets

A total of 30 protein sequences derived from the PB1-F2 gene (18 for H5N1, 7 for H9N2 and 5 for H1N1) were retrieved from GenBank.

Sequence alignment

PB1-F2 protein sequences of the selected strains were aligned using the program ClustalW [7] with default parameters.

Homology modelling

In the first step of homology modelling, a template structure related to these proteins was searched using Blast algorithms against PDB. The amino acids sequence of PB1-F2 protein of A/HK/156/97 was obtained from Swiss-Prot [ID: P0C0U0]. Homology modelling of PB1-F2 from A/

HK/156/97 (H5N1) based on the crystal structure of PB1-F2 protein [PDB id: 2HN8] from H1N1 subtypes with >69% identity, was carried out using Modeller [8]. The amino acid sequence of human ANT3 mitochondrial protein was retrieved from Swiss-Prot [ID: P12236]. The program Modeller9v4 was used to build a three-dimensional (3D) structure of human ANT3 using the X-ray crystal structure of bovine mitochondrial ANT2 ADP/ATP carrier protein [PDB id: 1OKC] having >80% identity as a template. The best models was chosen based on the dope score and used for further refinements.

Molecular dynamics and energy minimisation

Selected structures were refined by using energy minimisation and molecular dynamics techniques. At the first step, energy minimisation was performed using the CHARMm force field with steepest descent algorithm with 500 steps. Molecular dynamics of selected structures was carried out with periodic boundary condition under NVT ensemble. The system was maintained at 300 K. Molecular dynamics trajectories were propagated using the leap frog integration method. The SHAKE algorithm was used to constrain all bonds containing hydrogen atoms. All simulations were performed using the CHARMm package [9] with CHARMm force field. After simulation, energy minimisation of the selected structures was performed by CHARMm force field with steepest descent algorithm using 1,000 iterations at Accelrys Discovery Studio 2.0 [http://accelrys. com/products/discovery-studio]. Finally, validation of refined structures was performed by Procheck [10].

Docking studies

Rigid body docking of PB1-F2 protein with VDAC1 and ANT3 was performed by HEX5.1 [www.csd.abdn.ac.uk/hex]. Each docking solution was minimised by energy minimisation techniques. Details of interactions derived from refined structures were analysed using the LIGPLOT program [11].

Results and discussion

Comparative protein sequence analysis of PB1-F2 of H5N1, H9N2 and H1N1 subtypes

Multiple sequence analyses of the PB1-F2 protein of three subtypes (H1N1, H5N1 and H9N2) of IAV indicated that the PB1-F2 proteins among these subtypes were genetically related (Fig. 2). Nevertheless, the sequence similarities between the PB1-F2 sequence of the H1N1 isolate (A/Puerto Rico/8/34) and those of isolates H5N1 and H9N2 were only 57% to 66%, respectively. The human H5N1 isolate from the 1997 Hong Kong outbreak shared 57% to 60% similarity with the H1N1 strain of the 1934 outbreak. Furthermore, a secondary structure analysis was performed to gain functional insights into the PB1-F2 proteins of the selected subtypes. The secondary structure of PB1-F2 was predicted by NNPREDICT, SOPMA and PHD. All three programs strongly predict alpha helix from amino acids 55 to 63 and 70 to 83 (Figs. 2, 3). A helix found at the region 73–82 spans 11 amino acids and shows obvious similarity to the amphipathic alpha helix of the HTLV-I p13″ (human T-cell leukemia virus type 1) protein. This latter protein is known as a mitochondrial targetting protein [3, 12, 13].

Multiple sequence alignment showed that residues in the predicted helix were highly conserved among the three subtypes.

Homology modelling of PB1-F2 and ANT3 proteins

The PB1-F2 protein from the highly pathogenic H5N1 viruses isolated during the 1997 outbreak in Hong Kong was selected for modelling. A 3D structure was built based on PB1-F2 from H1N1 (PDB id: 2HN8A) using the Modeller9v4 program. Ramachandran plot analyses showed that 88.2% residues of PB1-F2 were in the most favourable region, 11.8% in the allowed region. The root mean squares deviation (RMSD) between the C-alpha atom of the template and the model was 0.89Å, indicating close homology. Thus the selected structure of PB1-F2 protein had a reasonable and reliable conformation and can be used for further simulation. The same procedure was applied for modelling the 3D structure of human ANT3 based on the crystal structure of ANT (PDB id: 1OKC). Ramachandran plot analyses (after minimisation) showed that >80% residues of the selected structure were in the most favoured region. RMSD between the model and template was 0.92Å, which again showed the close homology. Thus, both procheck and RMSD confirmed that both structures were reliable and can be used for further studies. The selected structures are depicted in Fig. 4a,b.

Protein–protein docking

The crystal structure of VDAC1 was downloaded from PDB (PDB id: 2K4T) and refined by energy minimisation and molecular simulation techniques. The program Hex5.1 was used to analyse the interaction between the C-terminal


Fig. 2 Alignment of PB1-F2 protein sequences of three different subtypes (H1N1, H5N1 and H9N2) of IAVs. Alignment was performed using the program ClustalW with default parameters. Amino acids conserved in >99% isolates are marked in *yellow*
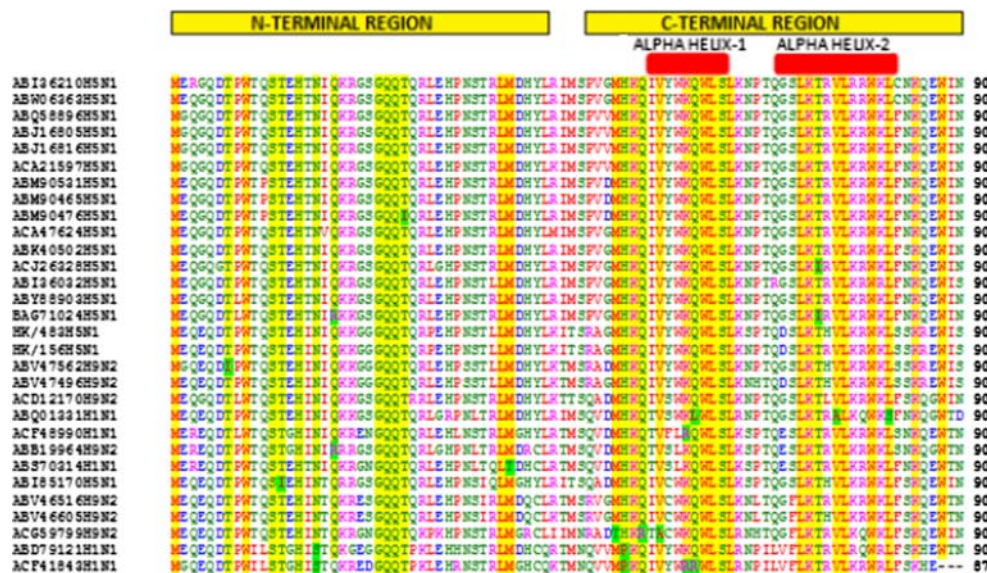
Fig. 3 Sequence alignment between PB1-F2 protein of A/HK/156/97 with the template (PDBID: 2HN8A) used in this study

region of the PB1-F2 protein with ANT3 and VDAC1. This program uses spherical polar Fourier correlation to accelerate docking calculations; the method is known to provide a feasible protein–protein docking orientation quickly and accurately [14]. Shape complementarity and electrostatic scoring representations were used to identify the best docked orientation. The complexes with best energy were chosen to analyse the key residues involve in hydrogen bonding and hydrophobic contacts. Figure 5a and Fig. 6a shows interactions of PB1-F2 protein with VDAC1 and ANT3 (mitochondrial membrane protein). The docking energies between PB1-F2 and the two mitochondrial membrane proteins VDAC1 and ANT3 were −772.82 and −455.76 kJ mol^{-1}, respectively (Table 1). Interaction energies in both complexes suggest that the PB1-F2
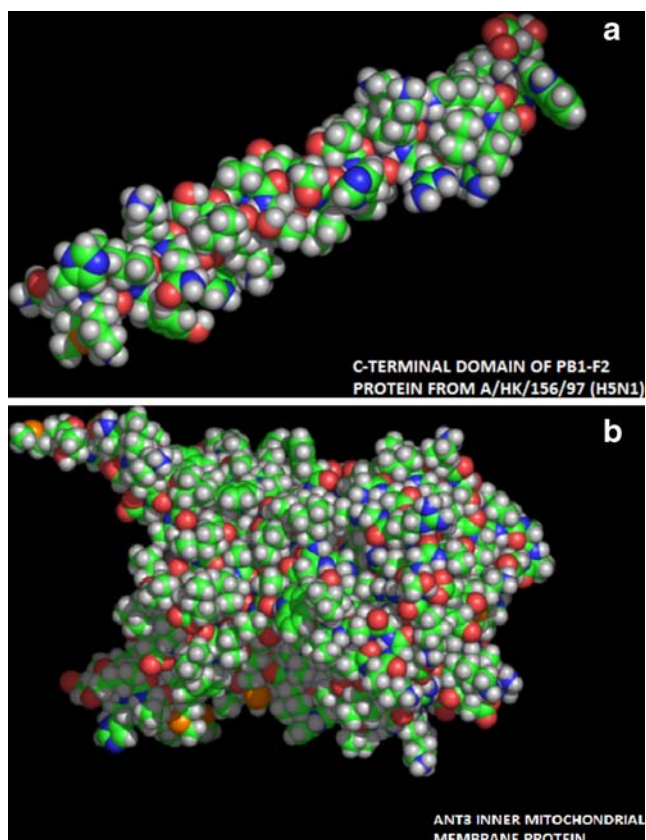

Fig. 4a,b CPK models. a Three dimensional (3D) structure of PB1-F2 protein from the H5N1 subtype occurring during the Hong Kong outbreak in 1997. b 3D structure of human ANT3
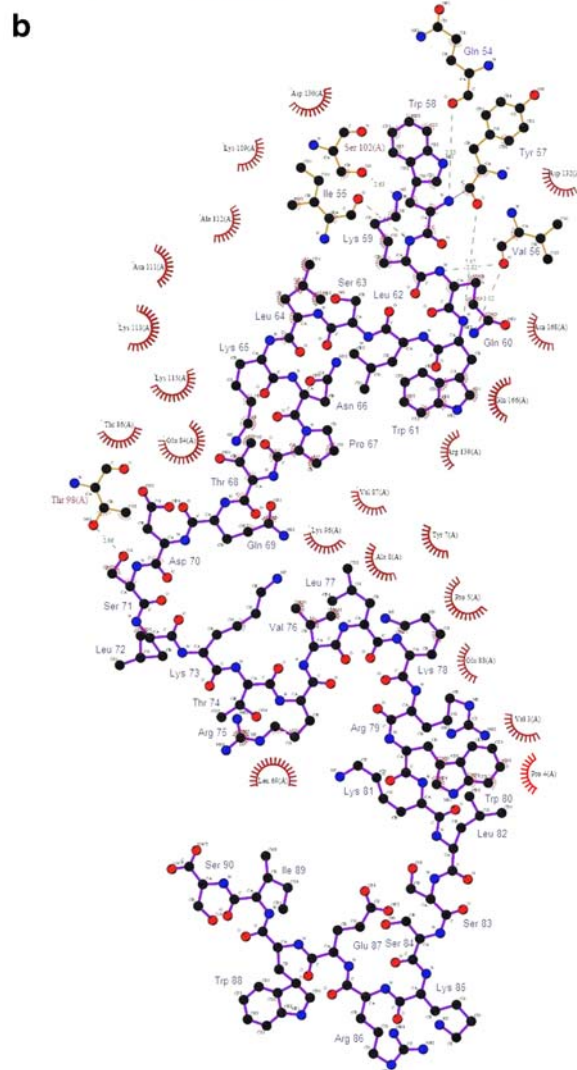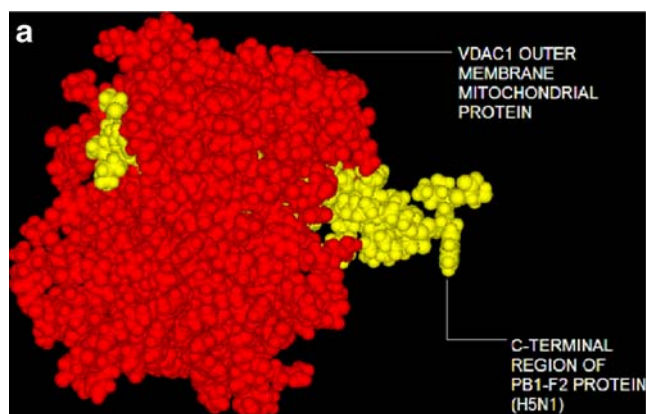
Fig. 5 a Docked complex of PB1-F2 and VDAC1. Both proteins are depicted as CPK models. b Schematic depiction of interactions between PB1-F2 and VDAC1 proteins generated by the Ligplot program

protein, through electrostatic interaction, forms a relatively stronger complex with VDAC1 as compared to ANT3 protein. However, in the case of the PB1-F2-ANT3 complex, shape complementarily score plays a significant
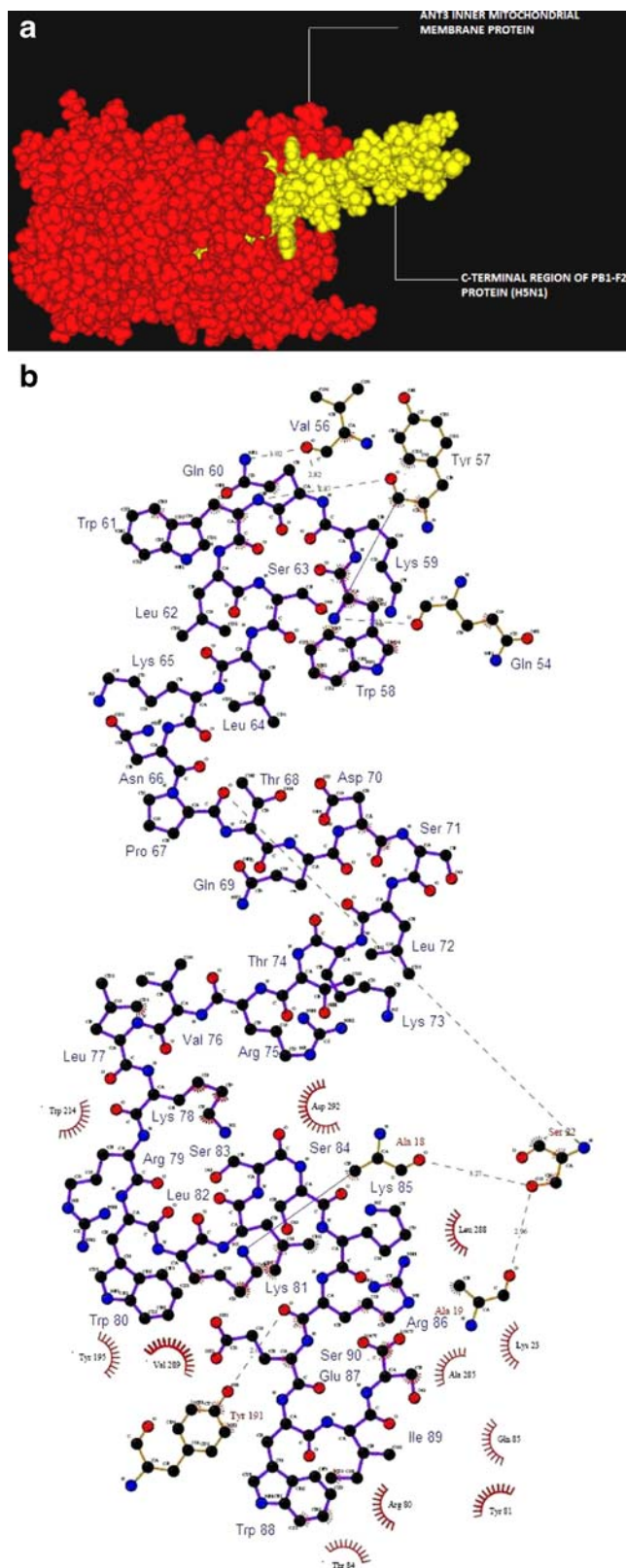
Table 1 Interaction energies in complexes. All energies are in kJ mol^{-1}

Complex	Etotal	Eshape	Eforce
PB1F2-VDAC1	−772.82	−722.32	−50.50
PB1F2- ANT3	−455.76	−427.21	28.55

role in maintaining stability (Table 1). In silico analyses using a docking program (Hex5.1) with molecular dynamics simulation revealed that the full length C-terminal region of PB1-F2 was able to interact with the interior region of VDAC1, whereas the MTS (mitochondrial targeting sequence) located near the COOH terminus was responsible for interacting with ANT3. Our findings are strongly supported by earlier studies showing that PB1-F2 protein with MTS targets the inner mitochondrial membrane [4].

Hydrogen bonding in PB1-F2- VDAC1 and PB1-F2- ANT3 complexes

Ligplot analyses depicted the involvement of two amino acids (Lys59 and Ser71) of PB1-F2 in the formation of hydrogen bonds with two amino acids [Ser102 (A) and Thr98 (A)] of VDAC1 protein (Fig. 5b). Residue Lys59, which form a hydrogen bond with Ser102 (A) with a distance of 2.63 Å, was found to be conserved among the three subtypes (except ACF48990 and ACF41843). However, Ser71 was able to make a hydrogen bond with Thr98 (A) with a distance of 2.66 Å. Ser71 is highly conserved in H5N1 isolates (Fig. 2) and helps in the formation of amphipathic alpha helix as predicted by three programs. Nevertheless, mutation of this amino acid (S→F; in three H9N2 strains, and two H1N1 strains) did not alter the secondary structure. In the case of the PB1-F2–ANT3 complex, two amino acids (Thr68 and Arg86) of PB1-F2 formed two hydrogen bonds with Ser22 and Tyr191of ANT3, with distances of 4.95 Å and 2.09 Å, respectively (Fig. 6b).

Hydrophobic interactions in PB1-F2–VDAC1 and PB1-F2–ANT3 complexes

The hydrophobic contact parameters of both complexes are listed in Tables 2 and 3.

A total of 13 amino acids of the PB1-F2 protein were able to make hydrophobic contacts with more than 20 amino acids of VDAC1, viz., 7 for Lys59 with Asn111(A), Ser102(A) and Lys109(A), with a distance of 2.77 Å to 3.67 Å; 4 for Gln60 with Asp132(A) and Asp130(A); 6 for Trp61 of PB1-F2 with Asn168(A) and Gln166(A) with 2.57 Å–3.82 Å distance; 2 for Lys65 with Ly113(A); 5 for

Fig. 6 **a** Docked complex of PB1-F2 and ANT3. Both the proteins are depicted as CPK models. **b** Schematic depiction of interactions between PB1-F2 and ANT3 protein generated by the Ligplot program

Table 2 Hydrophobic contacts between PB1-F2 and VDAC1 in the PB1-F2–VDAC1 complex

Total[a]	PB1-F2 residues	VDCA 1 residues	Distance (Å)
7	Lys59	Ser102, Lys109, Asn111	2.77-3.67
4	Gln60	Asp130, Asp132	3.28-3.85
6	Trp61	Gln166, Asn168	2.57-3.82
12	Leu64	Asn111, Ala112, Lys113	2.12-3.70
2	Lys65	Lys113	3.40-3.86
5	Pro67	Glu84	2.61-3.63
6	Thr68	Lys113, Lys115	2.46-3.54
2	Leu72	Lys115	3.25-3.32
1	Lys73	Ala8	3.72
15	Arg75	Leu69, Thr86, Val87, Glu88, Lys96	2.87-3.90
11	Val76	Pro5, Thr7, Ala8	2.29-3.84
3	Lys78	Leu69	3.36-3.83
10	Trp80	Val3, Pro4, Pro5	3.16-3.89

[a] Total hydrophobic contacts for PB1-F2 residue

Pro67 with Glu84(A) with 2.61Å–3.83Å; 6 for Thr68 with Lys115(A) and Lys113(A) with a distance of 2.46Å–3.54 Å; 2 for Leu72 with Lys115(A) with 3.25Å–3.32Å distance, 3 for Lys78 with Leu69(A) with 3.16Å–3.89Å. Lys73 has one hydrophobic contact with Ala8(A) of VDAC1. One important residue, Arg75 of PB1-F2 has 15 hydrophobic contacts with Leu69(A), Thr86(A), Val87(A), Glu88(A) and Lys96(A) of VDAC1 with distances of 2.87 Å–3.90Å (Table 2). Interaction of these amino acids of PB1-F2 protein is supported by experimental data, which showed that residues 63–75 along with Lys73 and Arg75 are crucial for mitochondrial targetting [3]. However, replacement of Lys73 and Arg75 residues with Ala completely abolished MTS function [4]. These conserved residues in the three subtypes (Fig. 2) were also found to be important in our study. Docking studies and structural optimisation found that residues Val76 and Trp80 of PB1-F2 have more then ten hydrophobic contacts with Pro4(A), Pro5(A), Tyr7(A), Ala8(A) and Val3(A) of VDAC1 with a distance of 2.29Å–3.89Å. Furthermore, 14 amino acids of ANT3 make 27 hydrophobic contacts with 9 amino acids of PB1-F2 protein, viz., 2 for Leu77 with Asp292(ANT3); 3 hydrophobic contacts for Lys78 (PB1-F2) with Val 289

(ANT3); 5 for Lys81 (PB1-F2) with Asp292, Leu288 and Ala18 of ANT3; 5 for Arg86 (PB1-F2) with Tyr 195 and Tyr 191 of ATN3 with distance of 3.47Å–3.90Å; 1 for Glu87 with Tyr191; 2 for Trp88 with Arg80 of ANT3 with a distance of 3.52Å–3.66Å, 1 for Ile89 with Gln85 (ANT3); 5 for Ser90 (PB1-F2) with Lys23, Ala19, Thr84 and Tyr81 of ANT3 with a distance of 3.23Å–3.76Å. Leu82 (PB1-F2) can make three hydrophobic contacts with three amino acids (Trp214, Val289 and Ala285) of ANT3 with distance of 3.05Å to 3.64Å (Table 3). Amino acid sequences LKTRVLKRWKL of PB1-F2 and LRVWRLCARRL of HTLV-I p13″—known mitochondrial localising proteins—have three Leu residues and are rich in basic amino acids [3, 12, 13]. These three Leu residues (Leu72, Leu77 and Leu82) are conserved among the three subtypes. The importance of these Leu residues can be highlighted by docking simulation, as Leu77 and Leu82 were able to make five hydrophobic contacts with four amino acids of ANT3 with distances of 2.63Å to 3.64Å (Table 3), and can play an important role in mitochondrial localisation. Experiments by Yamada et al. [6] showed that replacement of residues Lys and Arg at positions 78, 79 and 81 with Ala did not abolish mitochondrial targetting.

Table 3 Hydrophobic contacts between PB1-F2 and ANT3 in the PB1-F2–ANT3 complex

Total[a]	PB1-F2 residues	ANT3 residues	Distance (Å)
2	Leu77	Asp292	2.63-3.19
3	Lys78	Val289	2.01-3.77
5	Lys81	Ala18, Leu288, Asp292	3.44-3.87
3	Leu82	Trp214, Ala285, Val289	3.05-3.64
5	Arg86	Tyr195, Tyr191	3.47-3.90
1	Glu87	Tyr191	3.83
2	Trp88	Arg80	3.52-3.66
1	Ile 89	Gln85	3.23
5	Ser90	Ala19, Lys23, Tyr 81, Thr84	3.23-3.76

[a] Total hydrophobic contacts for PB1-F2 residue

Table 3 describes the binding of Lys78 and Lys81 with four amino acids of ANT3 by making eight hydrophobic contacts. Thus, our in silico findings suggest the significance of these residues (Lys78 and Lys81) in making favourable interactions with ANT3. Multiple sequence alignment showed that these residues are conserved (>98% in the isolates selected for this study) among the three subtypes and play an important role in forming the amphiphatic helix that is crucial for mitochondrial localisation (Fig. 2).

Conclusions

Comparative analyses and simulation studies revealed specific differences between PB1-F2–VDAC1 and PB1-F2–ANT3 complexes. The PB1-F2 protein was found to bind more strongly to VDAC1 than to ANT3 based on their interaction energies. Two alpha helices (regions 55–63 and 70–82) were found to be crucial for these interactions. Residues 63–75 along with Lys73 and Arg75, which are involved in mitochondrial targeting (as previously established experimentally), stabilised the PB1-F2–VDAC1 complex through hydrophobic contacts. The binding interactions identified from this study could be further validated experimentally. The interactions of PB1-F2 with VDAC1 and ANT3 can be further employed to design novel inhibitors against PB1-F2-induced apoptosis and will provide an interface for biochemical and pharmacological studies.

References

1. Khan AU (2006) Bioinformation 1(4):132–132
2. Chen W, Calvo PA, Malide D, Gibbs J, Schubert U, Bacik I, Basta SR, O'Neill, Schickli J, Palese P, Henklein P, Bennink JR, Yewdell JW(2001) Nat Med 7:1306–1312
3. Zamarin D, Ortigoza MB, Palese P (2006) J Virol 80:7976–7983
4. Zamarin D, Garcia-Sastre A, Xiao X, Wang R, Palese P (2005) P Los Pathog 1:e4
5. Gibbs JS, Malide D, Hornung F, Bennink JR, Yewdell JW (2003) J Virol 77:7214–7224
6. Yamada H, Chounan R, Higashi Y, Kurihara N, Kido H (2004) FEBS Lett 578:331–336
7. Thompson JD, Higgins DG, Gibson TJ (1994) Nucleic Acids Res 22:4673–4680
8. Sali A, Pottertone L, Yuan F, Vlijmen V, Karplus M (1995) Proteins 318-326
9. Brooks BR, Bruccoleri RE, Olafson BD, States DJ, Swaminathan S, Karplus M (1983) J Comp Chem 4:187–217
10. Laskowski RA, MacArthur MW, Moss DS, Thornton JM (1993) J Appl Cryst 26:283–291
11. Wallace AC, Laskowski RA, Thornton JM (1995) Protein Eng 8:127–134
12. Ciminale V, Zotti L, D'Agostino DM, Ferro T, Casareto L, Franchini G, Bernardi P, Chieco-Bianchi L (1999) Oncogene 18:4505–4514
13. D'Agostino DM, Zotti L, Ferro T, Franchini G, Chieco-Bianchi L, Ciminale V (2000) AIDS Res Hum Retrovir 16:1765–1770
14. Ritchie DW, Kemp GJL (2000) Proteins 39:178–194